Structure of high-spin states in ^{89}Sr and ^{90}Sr

E. A. Stefanova,[1,2] R. Schwengner,[1] G. Rainovski,[1,3] K. D. Schilling,[1] A. Wagner,[1] F. Dönau,[1] E. Galindo,[4] A. Jungclaus,[4] K. P. Lieb,[4] O. Thelen,[5] J. Eberth,[5] D. R. Napoli,[6] C. A. Ur,[7,*] G. de Angelis,[6] M. Axiotis,[6] A. Gadea,[8] N. Marginean,[6,*] T. Martinez,[6] Th. Kröll,[7] and T. Kutsarova[2]

[1]Institut für Kern- und Hadronenphysik, Forschungszentrum Rossendorf, D-01314 Dresden, Germany
[2]Institute for Nuclear Research and Nuclear Energy, BAS, 1784 Sofia, Bulgaria
[3]Faculty of Physics, University of Sofia, 1164 Sofia, Bulgaria
[4]II. Physikalisches Institut, Universität Göttingen, D-37073 Göttingen, Germany
[5]Institut für Kernphysik, Universität zu Köln, D-50937 Köln, Germany
[6]INFN, Laboratori Nazionali di Legnaro, I-35020 Legnaro, Italy
[7]INFN and Dipartimento di Fisica dell'Universita di Padova, I-35131 Padova, Italy
[8]Instituto de Fisica Corpuscular, E-46071 Valencia, Spain

(Received 15 February 2001; published 22 May 2001)

High-spin states of ^{89}Sr and ^{90}Sr were studied via the reactions ^{82}Se(^{11}B, $p3n$) and ^{82}Se(^{11}B, $p2n$), respectively, at a beam energy of 37 MeV. Gamma rays were detected with the GASP spectrometer. The level schemes of ^{89}Sr and ^{90}Sr were extended up to $E\approx 8$ MeV and $E\approx 10$ MeV, respectively. Level structures in ^{89}Sr and ^{90}Sr were interpreted in terms of the spherical shell model. The calculations were performed in the configuration space $(0f_{5/2},1p_{3/2},1p_{1/2},0g_{9/2})$ for the protons and $(1p_{1/2},0g_{9/2},1d_{5/2})$ for the neutrons. High-spin level sequences in ^{89}Sr are characterized by coupling the unpaired $d_{5/2}$ neutron to proton excitations of the core nucleus ^{88}Sr. An equidistant level sequence with $\Delta J=2$ found in ^{90}Sr is well described by the configuration $\pi[(0f_{5/2}^{-2})(0g_{9/2}^{2})]\nu(1d_{5/2}^{2})$ favoring even spins.

DOI: 10.1103/PhysRevC.63.064315 PACS number(s): 23.20.Lv, 25.85.Ge, 27.50.+e

I. INTRODUCTION

The nuclei $^{88-96}$Sr as well as $^{90-98}$Zr form the region of lowest collectivity of known nuclides between ^{56}Ni and the spherical Pb isotopes [1]. A value of $B(E2)=7.20(22)$ W.u. was adopted for the $2_1^+\rightarrow 0_1^+$ transition in the quasi-doubly magic nucleus $^{88}_{38}$Sr$_{50}$ [2]. Similarly low values of $B(E2)\approx 8$ W.u. and 13 W.u. were observed for the $2_1^+\rightarrow 0_1^+$ transitions in the chain of $^{90-94}$Sr ($N=52$–56) and in ^{96}Sr ($N=58$), respectively. Even lower values were reported for $^{92-98}$Zr ($N=52$–58) [1], whereas at $N=60$ a strong ground-state deformation of $\beta_2\approx 0.4$ was found [3]. The observed persistence of an almost constant nearly spherical ground-state shape for $50\leqslant N\leqslant 58$ in Sr and Zr isotopes was attributed to the subshell closures of low-j orbitals at $Z=38$,40 and $N=56$,58, which stabilize spherical configurations [1]. While the energies of the 2_1^+ states in the even Zr isotopes vary with the neutron number (2200, 935, 919, 1750, and 1223 keV for $N=50$–58, respectively), the energies of the 2_1^+ states in the Sr isotopes with $N=50$–58 remain almost constant at about 800 keV. The fact that the energy of the 2_1^+ state at the subshell closure at $N=56$ (^{94}Sr) does not reach roughly the energy of the 2_1^+ state (1836 keV) at $N=50$ (^{88}Sr) was related to a quenching of the $1p_{1/2}$-$1p_{3/2}$ proton spin-orbital splitting due to the neutron-proton interaction, as neutrons are added to the $1d_{5/2}$ neutron orbital [4]. As a result, proton excitations were proposed to contribute to the 2^+ states in ^{90}Sr and ^{92}Sr. A study of Sr isotopes between $N=50$ and $N=56$ could reveal whether such a quenching of the spin-orbital splitting of the $1p_{1/2}$-$1p_{3/2}$ proton orbitals may appear suddenly or gradually.

With this work, we continue our study of the high-spin structure of Sr isotopes, starting with the $N=50$ nucleus ^{88}Sr [5]. The nuclei ^{89}Sr and ^{90}Sr have one and two $1d_{5/2}$ neutrons, respectively, outside the shell closure at $N=50$. Thus, single-particle excitations are expected to dominate the structure of ^{89}Sr while an interplay of single-particle with vibrational-like states might occur in ^{90}Sr. So far, high-spin states of ^{89}Sr were investigated via ^{86}Kr(α,xn) reactions [6,7]. Excited states of ^{90}Sr were previously studied in β^--decay experiments (e.g., Ref. [8]), via (t,p) [9] and (^{6}Li, ^{8}B) [10] transfer reactions and recently in a fusion-fission experiment [11]. In the present work we establish the level schemes of ^{89}Sr and ^{90}Sr up to 8 and 10 MeV, respectively, and assign spin and parities to most of the levels.

II. EXPERIMENTAL METHODS AND RESULTS

Excited states of ^{89}Sr and ^{90}Sr were populated via the reactions ^{82}Se(^{11}B, $p3n$) and ^{82}Se(^{11}B, $p2n$), respectively, at a beam energy of 37 MeV. The ^{11}B beam was delivered by the XTU tandem accelerator of the Laboratori Nazionali di Legnaro. The target consisted of a 3.0 mg cm^{-2} layer of ^{82}Se enriched to 99.6% and evaporated on a 3 mg cm^{-2} gold backing. Gamma rays were detected with the GASP spectrometer [12] consisting of 40 escape-suppressed HPGe detectors and an inner ball containing 80 bismuth germanate elements. A total of 2.5×10^9 prompt γ-γ coincidence events were sorted off-line into E_γ-E_γ matrices and approxi-

*On leave from NIPNE Bucharest, Romania.

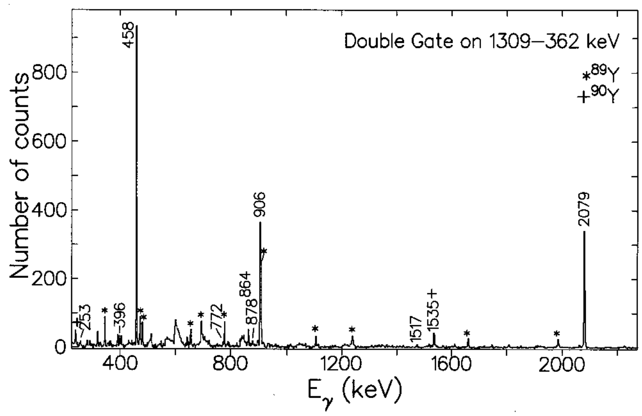

FIG. 1. Example of a double-gated background-corrected coincidence spectrum. Peaks labeled with their energy in keV are assigned to ^{89}Sr.

mately 3.8×10^8 γ-γ-γ events into an E_γ-E_γ-E_γ cube.

Based on a comparison of the intensities of the ground-state transitions we found that the relative cross sections of the channels leading to ^{89}Sr and ^{90}Sr amount to some 2% and 4%, respectively, of the strongest reaction channel ^{82}Se(^{11}B $4n$)^{89}Y. This strongest channel is predicted to include about 90% of the total cross section by the evaporation code PACE [13].

Double-gated spectra extracted from the cube using the code LEVIT8R [14] were analyzed to construct the level schemes of ^{89}Sr and ^{90}Sr. Examples of double-gated coincidence spectra for ^{89}Sr and ^{90}Sr, respectively, are shown in Figs. 1 and 2. Gamma rays assigned to ^{89}Sr and ^{90}Sr on the basis of the present experiment are listed in Tables I and II, respectively. Relative intensities were derived from coincidence spectra gated on the ground-state transitions, which were extracted from a E_γ-E_γ matrix including all detectors using the code VS [15].

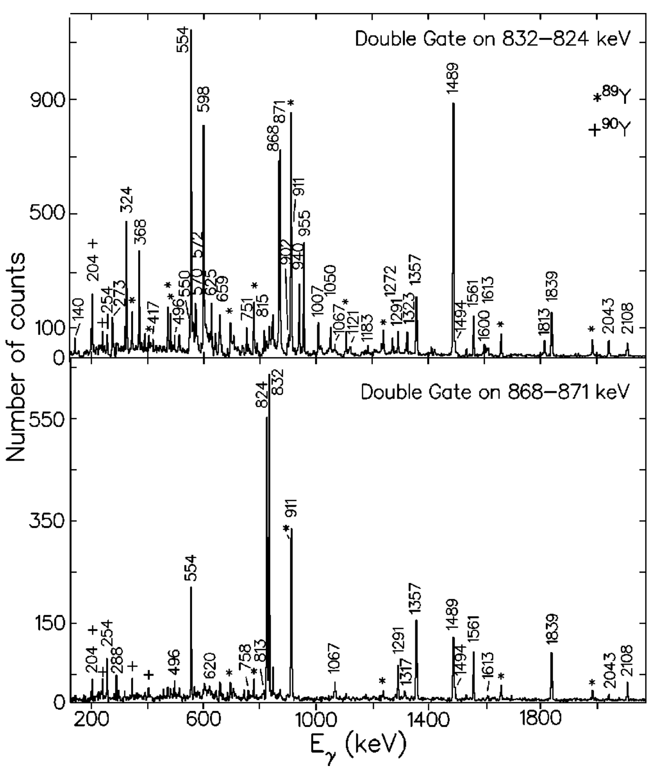

FIG. 2. Examples of double-gated background-corrected coincidence spectra. Peaks labeled with their energy in keV are assigned to ^{90}Sr.

TABLE I. Gamma rays assigned to ^{89}Sr in the present experiment.

E_γ [a] (keV)	I_γ [b]	R_{DCO} [c]	$\sigma\lambda$ [d]	J_i^π	J_f^π	E_i (keV)
253.3	0.5(1)			23/2		5979.1
283.9	1.6(1)	0.84(15)	$M1$	$15/2^-$	$15/2^-$	3672.6
362.4	44(1)	0.57(2)	$M1$	$17/2^-$	$15/2^-$	3751.1
395.9	1.5(2)[e]	0.34(10)[f]	($M1$)	(27/2)	(25/2)	7421.5
458.0	27.4(5)[e]		$M1/E2$[j]	$19/2^-$	$17/2^-$	4209.1
536.5	1.4(2)		$E2$	$19/2^-$	$15/2^-$	4209.1
771.7	1.7(2)		($M1$)	(27/2)	(25/2)	7421.5
820.4	25.8(4)	1.00(4)	$E2$	$19/2^-$	$15/2^-$	4209.1
864.0	5.5(5)	0.64(10)	$M1$ or $E1$	23/2	21/2	5979.1
878.3	1.1(4)	0.64(17)	$M1$ or $E1$	(25/2)	23/2	6857.4
906.0	33.6(9)	0.54(2)	$M1$ or $E1$	21/2	$19/2^-$	5115.1
1309.3	100(2)		$E2$[k]	$15/2^-$	$11/2^-$	3388.7
1334.5	0.7(2)				(25/2)	7984.3
1516.7	1.2(2)				$19/2^-$	5725.8
1534.7	13.1(6)[e]	1.10(4)[f] 1.88(9)[f,g] 1.36(6)[f,h] 1.57(6)[f,i]	($E2$)	(25/2)	21/2	6649.8
1593.2	1.2(1)		$E2$	$15/2^-$	$11/2^-$	3672.6
1910.5	1.2(1)		($E2$)	(25/2)	21/2	7025.6
2079.4	123(2)		$E3$[j]	$11/2^-$	$5/2^+$	2079.4

[a] γ-ray energy. The error is between 0.1 and 0.5 keV.

[b] Relative intensity derived from a spectrum gated by the 2079.4 keV transition and normalized to the 1309.3 keV transition.

[c] DCO ratio determined by gating on the 1309.3 keV $E2$ transition except for the cases *g*, *h*, and *i*.

[d] Multipolarity compatible with the DCO ratio and the deexcitation mode.

[e] Contaminated transition.

[f] Contaminated transition. The deduced DCO ratio may not be correct.

[g] DCO ratio determined by gating on the 362.4 keV $M1$ transition.

[h] DCO ratio determined by gating on the 820.4 keV $E2$ transition.

[i] DCO ratio determined by gating on the 906.0 keV $\Delta J=1$ transition.

[j] Taken from Ref. [7].

[k] Taken from Ref. [39].

A. Gamma-gamma directional correlations

Directional correlations of coincident γ rays from oriented states (DCO) provide information on the multipole order of the transitions and, thus, can be applied to assign spins to the emitting states. This method is described in detail in

TABLE II. Gamma rays assigned to ^{90}Sr in the present experiment.

E_γ[a] (keV)	I_γ[b]	R_{DCO}[c]	$\sigma\lambda$[d]	J_i^π	J_f^π	E_i (keV)
140.0	0.7(1)	0.44(5)	$M1$	$9^{(-)}$	$8^{(-)}$	5021.5
203.7	≈1[e]		($E1$)	$7^{(-)}$	$6^{(+)}$	3698.4
216.8	0.4(1)		($M1$)	$5^{(-)}$	(4^-)	3144.3
253.9	1.6(1)[e]	0.99(19)[i]	($E2$)			7959.5
272.5	3.5(1)	0.49(5)	$M1$	$9^{(-)}$	$8^{(-)}$	5021.5
288.3	1.0(1)	0.34(3)	$M1$ or $E1$			9060.5
324.0			($M1$)	$5^{(-)}$	$5^{(-)}$	3468.3
324.2	9.9(1)[f]	0.41(2)[f]	$M1$	$7^{(-)}$	$6^{(-)}$	4066.2
367.8	8.3(2)	0.95(6)	$M1$	$7^{(-)}$	$7^{(-)}$	4066.2
416.8	0.6(1)	0.40(4)	$M1$	$9^{(-)}$	$8^{(-)}$	5298.3
495.7	1.2(2)[e]	1.09(40)[i]	($E2$)	$6^{(+)}$	(4^+)	3764.2
549.6	2.4(2)	0.41(9)	$M1$	$9^{(-)}$	$8^{(-)}$	5298.3
554.1	33.6(6)	0.95(3)	$E2$	$7^{(-)}$	$5^{(-)}$	3698.4
570.2	4.8(4)	0.62(10)	$M1$	$10^{(-)}$	$9^{(-)}$	5591.7
571.5	1.4(4)		($E1$)	$7^{(-)}$	$6^{(+)}$	4066.2
597.7	16.9(4)[e,g]	0.62(2)[j]	$M1$	$6^{(-)}$	$5^{(-)}$	3742.0
597.9	5.5(2)[e,g]		($E2$)	$7^{(-)}$	$5^{(-)}$	4066.2
619.9	2.7(4)	0.33(26)	($E1$)	$6^{(+)}$	$5^{(-)}$	3764.2
625.1	5.5(4)	0.37(7)	($E1$)	$10^{(+)}$	$9^{(-)}$	5923.4
658.9	1.7(2)	0.64(8)	($M1$)	$13^{(-)}$	$12^{(-)}$	7371.1
720.5	1.4(1)	0.42(6)	$M1$	$4^{(-)}$	3^-	2927.5
751.2	3.1(1)	0.48(8)	$M1$	$12^{(-)}$	$11^{(-)}$	6712.2
757.8	1.1(1)	0.47(4)	$M1$ or $E1$			9957.3
812.7	0.3(1)[e]					8772.2
814.5	2.8(2)[e]	1.03(35)[i,j]	($E2$)	$6^{(-)}$	(4^-)	3742.0
824.2	92.3(2)	0.99(1)	$E2$[m]	4^+	2^+	1655.8
831.6	100(1)	0.98(2)	$E2$	2^+	0^+	831.6
868.0	25.7(5)	0.90(5)	$E2$	$10^{(+)}$	$8^{(+)}$	5923.4
871.0	24.7(5)	0.89(5)	$E2$	$12^{(+)}$	$10^{(+)}$	6794.4
		0.94(3)[k]				
901.9	2.1(2)		($E1$)	$10^{(+)}$	$9^{(-)}$	5923.4
911.2	14(1)[h]					7705.6
937.3	≈1[e]	0.85(10)	($E2$)	$5^{(-)}$	3^-	3144.3
939.5	9.3(2)	1.13(9)	$E2$	$11^{(-)}$	$9^{(-)}$	5961.0
955.3	14.7(2)	1.04(6)	$E2$	$9^{(-)}$	$7^{(-)}$	5021.5
1006.7	5.9(1)	1.01(8)	$E2$	$8^{(-)}$	$6^{(-)}$	4748.7
1050.3	5.1(3)	0.52(7)	$M1$	$8^{(-)}$	$7^{(-)}$	4748.7
1066.6	1.5(2)	0.94(10)	($E2$)			8772.2
1120.5	1.5(1)	0.90(18)[k]	$E2$	$12^{(-)}$	$10^{(-)}$	6712.2
		0.80(8)[l]				
1183.1	2.2(1)	0.34(10)	$M1$	$8^{(-)}$	$7^{(-)}$	4881.5
1271.7	2.6(1)[e]	0.78(12)[i]	($E1$)	(4^-)	4^+	2927.5
1291.2	4.6(1)	1.01(11)	$E2$	$8^{(+)}$	$6^{(+)}$	5055.4
1323.1	4.6(1)	1.02(13)	$E2$	$9^{(-)}$	$7^{(-)}$	5021.5
1357.0	14.1(3)	0.54(3)	($E1$)	$8^{(+)}$	$7^{(-)}$	5055.4
1375.4	2.7(2)	0.51(12)	$E1$	3^-	2^+	2207.0
1488.5	56.8(8)	0.51(1)	($E1$)	$5^{(-)}$	4^+	3144.3
1493.9	3.2(3)					9199.5
1560.7	9.8(2)	1.08(7)	$E2$	$8^{(+)}$	$6^{(+)}$	5055.4
1599.9	3.4(1)	0.92(7)	$E2$	$9^{(-)}$	$7^{(-)}$	5298.3
1612.8	2.1(1)[e]		($M1$)	(4^+)	4^+	3268.6
1812.5	4.7(1)	0.39(5)	($E1$)	$5^{(-)}$	4^+	3468.3
1838.9	12.0(2)[e]	0.81(4)	$E2$	$6^{(+)}$	4^+	3494.7
2042.6	6.5(1)	1.10(4)	($E3$)	$7^{(-)}$	4^+	3698.4
2108.4	3.3(1)		($E2$)	$6^{(+)}$	4^+	3764.2

[a] γ-ray energy. The error is between 0.1 and 0.5 keV.
[b] Relative intensity derived from a spectrum gated on the 824.2 keV transition and normalized to the 831.6 keV transition.
[c] DCO ratio determined by gating on the 824.2 keV transition except for the cases *j*, *k*, and *l*.
[d] Multipolarity compatible with the DCO ratio and the deexcitation mode.
[e] Contaminated transition.
[f] Unresolved doublet. A combined value derived for the doublet is given.
[g] Unresolved doublet. The intensity is estimated from coincidence spectra.
[h] This transition is strongly influenced by the intense 909 keV transition in ^{89}Y.
[i] Contaminated transition. The deduced DCO ratio may not be correct.
[j] DCO ratio determined by gating on the 1006.7 keV transition.
[k] DCO ratio determined from a sum spectrum gated on the 824.2 and 831.6 keV transitions.
[l] DCO ratio determined by gating on the 554.1 keV transition.
[m] Taken from Ref. [9].

Refs. [16–18]. To deduce the DCO ratios, γ-γ events with one γ ray detected in one of the 12 detectors placed at 31.7°, 36.0°, 144.0°, and 148.3° and the other one detected in one of eight detectors at 90° relative to the beam direction were sorted into a coincidence matrix. Coincidence spectra were extracted by applying gates on certain peak and background intervals in the (35°, 90°) matrix and in the transposed (90°, 35°) matrix. The DCO ratios were obtained as the ratio of peak intensities in both background-corrected spectra. The coincidence spectra and the peak intensities were extracted using the code VS [15]. A DCO ratio of 1.0 is expected if the gating and the observed transitions are stretched transitions of pure and equal multipole order. For the present detector geometry and completely aligned nuclei, a value of 0.54 is expected for a pure dipole transition gated on a stretched quadrupole transition. A value of 1.0 or 1.85 is expected for a $\Delta J=0$ transition using a gate on a

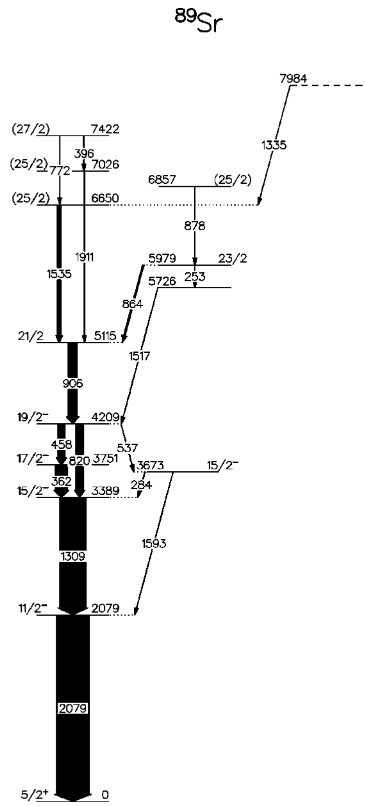

FIG. 3. Level scheme of ^{89}Sr deduced from the present experiment.

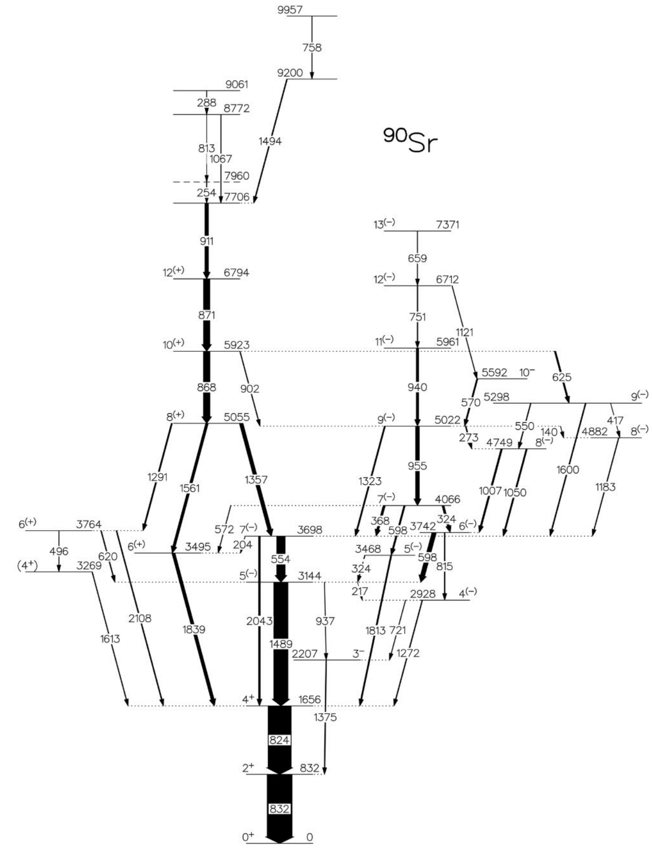

FIG. 4. Level scheme of ^{90}Sr deduced from the present experiment.

$\Delta J=2$ or $\Delta J=1$ transition, respectively. The resulting DCO ratios for ^{89}Sr and ^{90}Sr are given in Tables I and II, respectively.

B. The level scheme of ^{89}Sr

The level scheme of ^{89}Sr deduced from the present experiment is shown in Fig. 3. It has previously been known up to the $(19/2^-)$ state at 4209 keV [7]. In the present experiment, two new level sequences above this state have been observed as well as a new 536.5 keV transition linking the 3673 and 4209 keV levels. We propose $J^\pi=15/2^-$ for the 3673 keV level on the basis of the DCO ratio of the 283.9 keV transition (cf. Table I) and the observation of the 536.5 keV transition. This is not consistent with the assignment of $J^\pi=13/2^-$ given in Ref. [7]. Based on the dipole character of the 362.4 keV γ ray and the quadrupole character of the 820.4 keV transition, we assign $J^\pi=17/2^-$ and $19/2^-$ to the 3751 and 4209 keV levels, respectively, which confirms the tentative assignments in Ref. [7]. The DCO ratios of the 906.0 and 864.0 keV transitions (see Table I) indicate dipole character. Thus, we assign $J=21/2$ and $J=23/2$ to the 5115 and 5979 keV levels, respectively. The 1534.7 keV transition is superimposed by the 1535 keV transition in ^{90}Y. Therefore, we propose tentatively $J=(25/2)$ for the 6650 keV level. Based on DCO ratios and deexcitation characteristics, tentative assignments of $J=(25/2)$, $(25/2)$, and $(27/2)$ are proposed for the 6857, 7026, and 7422 keV levels, respectively.

In the present experiment, a thick target (see Sec. II) was used to stop the recoil nuclei and, thus, to enable an analysis of level lifetimes applying the Doppler-shift-attenuation (DSA) method. However, no Doppler shift was observed for any transition depopulating the states up to the 5115 keV level in ^{89}Sr. This means that the effective lifetimes of the corresponding levels are greater than about 5 ps. The transitions depopulating higher-lying states are too weak for a line-shape analysis.

C. The level scheme of ^{90}Sr

The level scheme of ^{90}Sr deduced from the present experiment is shown in Fig. 4. It has been known from previous in-beam studies up to the 3144 keV level [8,9]. During our study we became aware of a fusion-fission experiment showing level sequences up to the 5961 and 7706 keV levels, respectively, and published in conference proceedings [11]. In addition to that work, we establish new levels on top of the 5961 and 7706 keV levels as well as new levels at 3269, 3468, 4882, 5298, and 5592 keV and observe 17 new transitions. Moreover, we make spin and parity assignments for most of the levels on the basis of the present DCO analysis and deexcitation modes.

For the lowest levels at 832, 1656, and 2207 keV spin and parity assignments of 2^+, 4^+, and 3^-, respectively, were made in Refs. [9,19]. A level at 3144.9 keV was observed in the β^- decay of the 3^- state in ^{90}Rb [8]. The value of $\log f_1 t = 9.9$ (i.e., >8.5), calculated from the $\log ft$ value of the populating transitions [8] is compatible with the first forbidden unique transition ($\Delta J=2$, $\pi=-1$) and, thus, consistent with a spin and parity assignment of 5^+ for the 3145 keV state. On the other hand, a 3146 keV level was observed in a (t,p) reaction [9], where $J^\pi=(5^-)$ was proposed. In the present experiment, a DCO ratio consistent with dipole character was obtained for the 1488.5 keV transition (see Table II). Thus, we confirm the spin assignment $J=5$ for the 3144 keV level. This is also consistent with the quadrupole character of the 937.3 keV transition populating the 3^- state at 2207 keV. Although multipolarity $M2$ cannot be totally excluded for the weak 937.3 keV transition, we consider this unlikely and assume multipolarity $E2$. This assumption results in the tentative assignment of negative parity to the $J=5$ state at 3144 keV. Analogously, we assume multipolarity $E2$ for the 554.1 keV quadrupole transition populating the $5^{(-)}$ state, and propose a tentative assignment of $J^\pi=7^{(-)}$ for the level at 3698 keV. According to the discussed assignments, the 2042.6 keV transition has multipolarity $E3$. Analogous $E3$ transitions were observed with energies of 2734 keV ($3^-\rightarrow 0^+$) in ^{88}Sr [2] and 2079 keV ($11/2^-\rightarrow 5/2^+$) in ^{89}Sr (see Fig. 3).

In the (t,p) study [9], tentative assignments of 3^- or 4^+ were proposed for a 3268 keV state, which may correspond to the 3269 keV state observed in this work. Spin and parity 3^- seem, however, rather unlikely. We propose tentatively spin and parity (4^+). On the basis of the quadrupole character of the 1838.9, 1291.2, 1560.7, 868.0, and 871.0 keV transitions (cf. Table II) we assign $J^\pi=6^{(+)}$, $6^{(+)}$, $8^{(+)}$, $10^{(+)}$, and $12^{(+)}$ for the 3495, 3764, 5055, 5923, and 6794 keV states, respectively. The dipole character of the 1357.0 keV transition is consistent with the spin assignments of $J=7$ and $J=8$ for the 3698 and 5055 keV states, respectively. The DCO ratio of the 911.2 keV transition could not be deduced due to the interference with the intense 909 keV transition in ^{89}Y. The DCO ratios of the 253.9 and 1066.6 keV transitions point to $\Delta J=0$ or $\Delta J=2$ transitions, while the DCO ratios of the 288.3 and 757.8 keV transitions are consistent with dipole character.

Based on the quadrupole character of the 955.3, 1323.1, 1599.9, and 939.5 keV transitions (see Table II) negative parity may be tentatively proposed for the 4066, 5022, 5298, and 5961 keV levels, respectively. We also tentatively assume negative parity for the 4749 and 4882 keV states. The multipole orders of all linking transitions are consistent with the proposed spin assignments. Based on the $J^\pi=8^{(-)}$ assignment for the 4749 keV state and on the $\Delta J=2$ character of the 1006.7 keV transition, spin and parity of $J^\pi=6^{(-)}$ for the 3742 keV state can be tentatively assigned. This is in agreement with the dipole character of the 597.7 keV transition depopulating the 3742 keV state to the 3144 keV state. The DCO ratios deduced for the 720.5, 814.5, and 1271.7 keV transitions are consistent with $J^\pi=4^{(-)}$ for the 2928 keV state. The DCO ratio of the 1812.5 keV transition indicates a $\Delta J=1$ transition, which results in the assignment of $J=5$ for the 3468 keV level. Since multipolarity $M2$ is unlikely for the populating 597.9 keV transition, we suggest negative parity for the 3468 keV state as well.

In the present thick-target experiment, no Doppler shift was observed for any transition in ^{90}Sr. Accordingly, the effective lifetimes of the levels up to the 7706 keV are greater than about 5 ps. The transitions depopulating higher-lying levels are, however, too weak to observe a line shape.

III. DISCUSSION

A. Shell-model calculations for ^{89}Sr and ^{90}Sr

Shell-model studies of nuclei with $N>50$ were focused during the last years on nuclei with $Z>40$. In these studies a model space including the $1p_{1/2}$, $0g_{9/2}$ orbitals for the protons and the $1d_{5/2}$, $2s_{1/2}$ orbitals for the neutrons has been used. The states with spins up to $J\approx 15$ could be well described within this model space for, e.g., the $N=51$ nuclei ^{94}Tc [20] and ^{95}Ru [21] and for the $N=52$ nuclei ^{94}Mo [22] and ^{96}Ru [23], whereas the description of states with higher spins is improved with an extended model space including the higher-lying neutron orbitals $0g_{7/2}$, $1d_{3/2}$, and $0h_{11/2}$ as well as excitations of $0g_{9/2}$ neutrons across the $N=50$ shell gap into the $1d_{5/2}$ orbital [20,22,23].

In the Sr isotopes with $Z=38$, excitations of $0f_{5/2}$ or $1p_{3/2}$ protons to the $1p_{1/2}$, $0g_{9/2}$ orbitals may contribute to the configurations of high-spin states. The model space used in our calculations includes the active proton orbitals $(0f_{5/2},1p_{3/2},1p_{1/2},0g_{9/2})$ and neutron orbitals $(1p_{1/2},0g_{9/2},1d_{5/2})$ relative to a hypothetical ^{66}Ni core. The restricted neutron space should be adequate for the description of states up to $J\approx 15$. Since an empirical set of effective interactions for this model space is not available up to now, various empirical interactions have been combined with results of schematic nuclear interactions by applying the surface delta interaction. Details of this procedure are described in Refs. [24–27]. The effective interaction in the proton shells was taken from Ref. [28]. In that work the residual interaction and the single-particle energies of the proton orbitals were deduced from a least-squares fit to 170 experimental level energies in $N=50$ nuclei with mass numbers between 82 and 96. The data given in Ref. [29] have been used for the proton-neutron interaction between the $\pi(1p_{1/2},0g_{9/2})$ and the $\nu(1p_{1/2},0g_{9/2})$ orbitals. These data were derived from an iterative fit to 95 experimental level energies of $N=48$, 49, and 50 nuclei. The matrix elements of the neutron-neutron interaction of the $\nu(1p_{1/2},0g_{9/2})$ orbitals have been assumed to be equal to the isospin $T=1$ component of the proton-neutron interaction given in Ref. [29]. For the $(\pi 0f_{5/2},\nu 0g_{9/2})$ residual interaction the matrix elements proposed in Ref. [30] have been used. The single-particle energies relative to the ^{66}Ni core used here were derived from the single-particle energies of the proton orbitals given in Ref. [28] with respect to the ^{78}Ni core and from the neutron single-hole energies of the $1p_{1/2},0g_{9/2}$ orbitals [29]. The transformation of these single-particle energies to those relative to the ^{66}Ni core has been performed [31] on the basis of the effective residual interactions given above. The obtained values are $\epsilon^{\pi}_{0f_{5/2}}=-9.106$ MeV, $\epsilon^{\pi}_{1p_{3/2}}=-9.033$ MeV, $\epsilon^{\pi}_{1p_{1/2}}=-4.715$ MeV, $\epsilon^{\pi}_{0g_{9/2}}=-0.346$ MeV, $\epsilon^{\nu}_{1p_{1/2}}=-7.834$

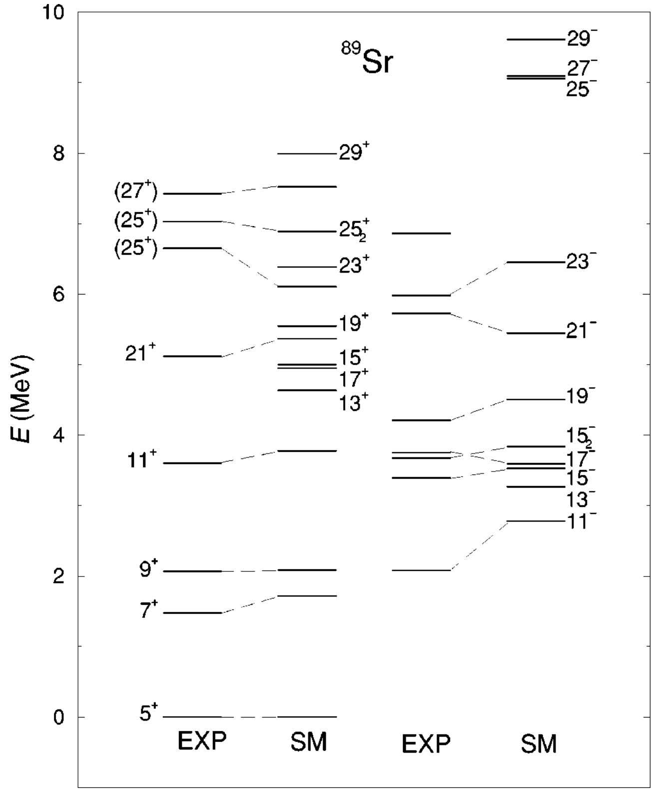

FIG. 5. Comparison of experimental with calculated level energies in ^{89}Sr. Spins are given as $2J$.

MeV, $\epsilon^{\nu}_{0g_{9/2}}=-6.749$ MeV, and $\epsilon^{\nu}_{1d_{5/2}}=-4.144$ MeV. These single-particle energies and the corresponding values for the strengths of the residual interactions have been used to calculate level energies as well as $M1$ and $E2$ transition strengths. For the latter, effective g factors of $g_s^{\rm eff}=0.7g_s^{\rm free}$ and effective charges of $e_\pi=1.72e, e_\nu=1.44e$ [32], respectively, have been applied.

The nuclei ^{89}Sr or ^{90}Sr have ten protons and 13 or 14 neutrons, respectively, in the considered configuration space. To make the calculations feasible a truncation of the occupation numbers has been applied. At most four protons are allowed to occupy the $(1p_{1/2},0g_{9/2})$ subshell. Two of the neutrons are assumed to occupy the $1p_{1/2}$ orbital and ten the $0g_{9/2}$ orbital while the remaining one or two appear in the $1d_{5/2}$ orbital for ^{89}Sr or ^{90}Sr, respectively. Excitations of neutrons from the $0g_{9/2}$ orbital to the $1d_{5/2}$ orbital are neglected. With these restrictions configuration spaces with dimensions smaller than 10 200 have been obtained. The calculations were carried out using the code RITSSCHIL [33].

B. Results for ^{89}Sr

Calculated level energies of states in ^{89}Sr are compared with experimental ones in Fig. 5. The experimental $7/2^+$, $9/2^+$, and $11/2^+$ states observed in Ref. [7] but not in the present experiment are also included in Fig. 5.

The $5/2^+$ ground state is dominated by the unpaired $1d_{5/2}$ neutron. The calculated lowest-lying $7/2^+$ and $9/2^+$ states are generated mainly by breaking a $1p_{3/2}$ proton pair and lifting one proton to the $1p_{1/2}$ orbital. The resulting configuration $\pi(1p^{-1}_{3/2}1p^{1}_{1/2})\nu(1d^{1}_{5/2})$ is exhausted at $J=9/2$. Calculated $M1$ and $E2$ transition strengths are compared with experimental values in Table III. The predicted $M1$ strength of the $7/2^+\rightarrow5/2^+$ transition and the $E2$ strength of the $9/2^+\rightarrow5/2^+$ transition reproduce the experimental values while the calculated $B(M1,9/2^+\rightarrow7/2^+)$ value exceeds the experimental one by a factor of about 8. The calculated lowest lying $11/2^+$ state contains mainly the configuration $\pi(0f^{-1}_{5/2}1p^{1}_{1/2})\nu(1d^{1}_{5/2})$. The positive-parity states with higher spin up to $J=29/2$ include the excitation of two protons into the $0g_{9/2}$ orbital, i.e., configurations of the type $\pi[(0f^{-1}_{5/2}1p^{-1}_{3/2})_{J_{fp}}(0g^{2}_{9/2})_{J_g}]\nu(1d^{1}_{5/2})$ with $J_{fp}=2,4$ and $J_g=0,8$ or of the type $\pi[(0f^{-2}_{5/2})_{J_f}(0g^{2}_{9/2})_{J_g}]\nu(1d^{1}_{5/2})$ with $J_f=0,2,4$, and $J_g=6,8$.

The experimental levels at 5115, 6650, 7026, and 7422 keV are suggested to correspond to the calculated $21/2^+_1$, $25/2^+_1$, $25/2^+_2$, and $27/2^+_1$ states, respectively. The comparison of level sequences in ^{88}Sr and ^{89}Sr given in Fig. 6 shows that the level spacings between the 4209, 5115, 6650, 7026, and 7422 keV levels in ^{89}Sr resemble those between the 7^-, 8^+, 10^+_1, 10^+_2, and 11^+ states in ^{88}Sr. This may indicate that the considered states in ^{89}Sr arise from a coupling of the unpaired $1d_{5/2}$ neutron to the respective core states. Indeed, the main component of the wave function of the calculated $21/2^+$ state corresponds to the coupling of a $d_{5/2}$ neutron to the main component of the 8^+ state in the core nucleus ^{88}Sr [5,34]. The $25/2^+$ state is calculated lower in energy than the $23/2^+$ state, which is compatible with the observation of a (25/2) state as the next on top of the 21/2 state. The calculated $25/2^+$ state in ^{89}Sr is almost 0.5 MeV lower than the experimental (25/2) state at 6650 keV as the calculated 10^+_1 state in ^{88}Sr is about 1 MeV lower than the experimental 10^+ state in ^{88}Sr [5]. The 7026 and 7422 keV levels in ^{89}Sr may correspond to the calculated $25/2^+_2$ and $27/2^+_1$ states, respectively.

The negative-parity states in ^{89}Sr up to the $19/2^-$ state at 4209 keV were proposed to result from coupling the unpaired $1d_{5/2}$ neutron to the lowest-lying 3^-, 5^-, 6^-, and 7^- states in the core nucleus ^{88}Sr in Ref. [7]. This interpretation, which is analogous to the above discussion of the positive-parity states, was confirmed by cluster-phonon-model calculations [35] and is consistent with the predictions of the

TABLE III. Experimental and calculated transition strengths in ^{89}Sr.

$J^\pi_{\rm i}$	$J^\pi_{\rm f}$	$B(M1)_{\rm exp}$ [a] (W.u.)	$B(M1)_{\rm SM}$ [b] (W.u.)	$B(E2)_{\rm exp}$ [a] (W.u.)	$B(E2)_{\rm SM}$ [b] (W.u.)
$7/2^+_1$	$5/2^+_1$	$0.017^{+0.011}_{-0.004}$ [c]	0.027	$4.6^{+2.4}_{-1.3}$ [c]	8.8
$9/2^+_1$	$7/2^+_1$	0.050(15) [c]	0.40		
$9/2^+_1$	$5/2^+_1$			$2.7^{+1.1}_{-0.6}$ [c]	4.4

[a]Experimental reduced transition strengths in Weisskopf units (W.u.). 1 W.u.$(M1)=1.79\ \mu_N^2$, 1 W.u.$(E2)=23.60e^2{\rm fm}^4$.
[b]Calculated reduced transition strengths in Weisskopf units. Values of $g_s^{\rm eff}=0.7g_s^{\rm free}$ and $e_\pi=1.72e, e_\nu=1.44e$ were used for the $B(M1)$ and $B(E2)$ values, respectively.
[c]Value taken from Ref. [7].

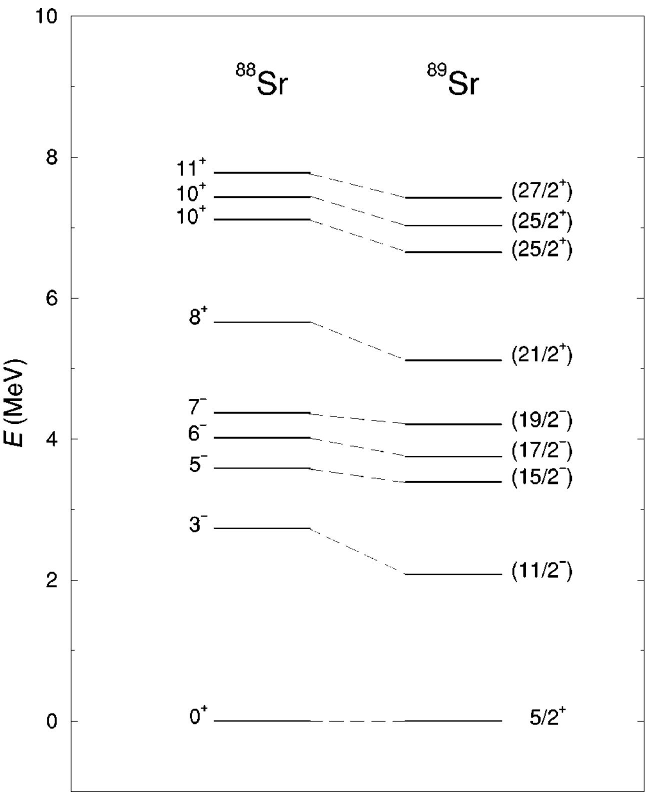

FIG. 6. Comparison of experimental level energies in ^{88}Sr with ^{89}Sr.

present shell-model calculations. The $11/2^-$ and $15/2^-$ states are described by the unpaired $1d_{5/2}$ neutron and by breaking up a $1p_{3/2}$ proton pair and lifting one proton into the $0g_{9/2}$ orbital, leading to the configuration $\pi(1p_{3/2}^{-1}0g_{9/2}^{1})\nu(1d_{5/2}^{1})$, while in the $13/2^-$, $15/2_2^-$, $17/2^-$, and $19/2^-$ states the configuration $\pi(0f_{5/2}^{-1}0g_{9/2}^{1})\nu(1d_{5/2}^{1})$ predominates. The calculated lowest-lying $11/2^-$ state is about 700 keV higher than the experimental one. A previous (d,p) study [36] suggested that an admixture of the $\nu(0h_{11/2})$ orbital to the $11/2^-$ state lowers its energy relative to the undisturbed one. However, this is not included in the present model space. The creation of the $21/2^-$ and $23/2^-$ states requires the breakup of a further proton pair resulting in the configuration $\pi[(0f_{5/2}^{-1}1p_{3/2}^{-1})_4 1p_{1/2}^{1}0g_{9/2}^{1}]\nu(1d_{5/2}^{1})$. These two states may be related with the experimental levels at 5726 and 5979 keV, respectively.

To generate negative-parity states with even higher spin it is necessary to excite three protons to the $0g_{9/2}$ orbital. This causes an energy gap of about 2.5 MeV between the $23/2^-$ state, and the $25/2^-$ to $29/2^-$ states dominated by the configuration $\pi[(0f_{5/2}^{-2}1p_{3/2}^{-1})_{J_{fp}}(0g_{9/2}^{3})_{J_g}]\nu(1d_{5/2}^{1})$ with $J_{fp}=1/2$, 5/2, and $J_g=17/2$, 21/2. If one assumes negative parity for the sequence of levels at 5726, 5979, and 6857 keV, then the 6857 keV level is not compatible with the predicted gap between the $23/2^-$ and $25/2^-$ states. In this case, neutron orbitals not included in the present calculations as $0g_{7/2}$ might play a role. The $\pi[(0f_{5/2}^{-1}1p_{3/2}^{-1})_4 1p_{1/2}^{1}0g_{9/2}^{1}]\nu(0g_{7/2}^{1})$ configuration, e.g., can generate a negative-parity state with a maximum spin of 25/2. At higher spin, negative-parity states including neutron-core excitations might also appear as it was predicted for states with $J\geqslant 13$ and $J\geqslant 23/2$ in ^{94}Mo ($Z=42,N=52$) and ^{95}Mo ($N=53$), respectively [22].

C. Results for ^{90}Sr

Experimental and calculated level energies in ^{90}Sr are shown in Fig. 7. The main components of the shell-model positive-parity and negative-parity states are listed in Tables IV and V, respectively.

The calculated lowest-lying 0^+, 2^+, and 4^+ states are mainly characterized by the $\nu(1d_{5/2}^{2})_J$ excitation with $J=0,2,4$, respectively. As a consequence of the proposed quenching of the proton $1p_{3/2}-1p_{1/2}$ spin-orbital splitting in the Sr isotopes, as neutrons are added to the $1d_{5/2}$ orbital (see Introduction), the contribution of proton configurations was discussed in Ref. [4] for the first 2^+ states in ^{90}Sr and ^{92}Sr. Indeed, proton contributions of about 8% and 2% are predicted for the first 2^+ and 4^+ states, respectively, in ^{90}Sr in the present calculations. The predicted $E2$ strengths of the $2^+\rightarrow 0^+$ and $4^+\rightarrow 2^+$ transitions agree well with the experimental values as can be seen in Table VI. However, the calculated states form a multipletlike sequence as observed in the $N=52$ isotone ^{92}Zr [37,38], while the experimental states display rather a vibrational behavior, although the experimental $B(E2)$ values decrease with increasing spin. The discrepancy between the experimental and calculated energies of the 4_1^+ state may cause similar discrepancies for high-spin states that include analogous configurations, i.e., a coupling of the $(1d_{5/2}^{2})_4$ neutrons to excitations of the proton system.

To generate a 5^+ state it is necessary to break a pair. Thus, the main configuration for the 5^+ and 6^+ states is $\pi(1p_{3/2}^{-1}1p_{1/2}^{1})_2\nu(1d_{5/2}^{2})_4$, while $\pi(0f_{5/2}^{-1}1p_{1/2}^{1})_{2,3}\nu(1d_{5/2}^{2})_4$ is predicted for the 6_2^+ and 7^+ states. The energy difference of 2067 keV between the calculated 4_1^+ and 6_1^+ states is close to the experimental value of 1839 keV between the 4_1^+ state and the $6^{(+)}$ state at 3495 keV. This level spacing is also close to the energy of the first 2^+ state at 1836 keV in ^{88}Sr, which has the main configuration $\pi(1p_{3/2}^{-1}1p_{1/2}^{1})$. Thus, no apparent quenching of the $1p_{3/2}$-$1p_{1/2}$ proton spin-orbital splitting [4] can be concluded for ^{90}Sr from this rough estimate. The calculated 6^+ state is lower than the experimental one by about 500 keV, which is close to the difference between the experimental and calculated 4_1^+ states (see Fig. 7). Thus, this difference may be related with the analogous configurations in these states (see Table IV) as discussed above. The second 6^+ state is calculated about 3.4 MeV above the first 4^+ state, whereas the difference of the corresponding experimental states is only about 2.1 MeV. This discrepancy might be caused by configurations not included in the present model space as neutron excitations of the type $\nu(1d_{5/2}^{1}0g_{7/2}^{1})$.

The calculated 8^+ to 16^+ states include the excitation of two protons into the $0g_{9/2}$ orbital. The main configuration of the calculated first 8^+ to 12^+ states is $\pi[(0f_{5/2}^{-2})_{J_f}(0g_{9/2}^{2})_{J_g}]\nu(1d_{5/2}^{2})_{J_d}$ with $J_f=0$, $J_g=6,8$ and $J_d=0,2,4$. The calculated 13^+ and 16^+ states are dominated by the configurations

TABLE IV. Main components of wave functions of positive-parity states in ^{90}Sr.

J^{π}	Configuration[a]	v[b]	A[c]
2_1^+	$\nu(1d_{5/2}^2)_2$	2	47
4_1^+	$\nu(1d_{5/2}^2)_4$	2	52
4_2^+	$\pi(1p_{3/2}^{-1}1p_{1/2}^1)_2\nu(1d_{5/2}^2)_2$	4	40
4_3^+	$\pi(1p_{3/2}^{-1}1p_{1/2}^1)_2\nu(1d_{5/2}^2)_4$	4	40
5_1^+	$\pi(1p_{3/2}^{-1}1p_{1/2}^1)_2\nu(1d_{5/2}^2)_4$	4	78
6_1^+	$\pi(1p_{3/2}^{-1}1p_{1/2}^1)_2\nu(1d_{5/2}^2)_4$	4	80
6_2^+	$\pi(0f_{5/2}^{-1}1p_{1/2}^1)_2\nu(1d_{5/2}^2)_4$	4	33
7_1^+	$\pi(0f_{5/2}^{-1}1p_{1/2}^1)_3\nu(1d_{5/2}^2)_4$	4	71
8_1^+	$\pi[(0f_{5/2}^{-2})_0(0g_{9/2}^2)_8]\nu(1d_{5/2}^2)_0$	2	11
9_1^+	$\pi[(0f_{5/2}^{-2})_0(0g_{9/2}^2)_8]\nu(1d_{5/2}^2)_2$	4	10
10_1^+	$\pi[(0f_{5/2}^{-2})_0(0g_{9/2}^2)_6]\nu(1d_{5/2}^2)_4$	4	16
10_2^+	$\pi[(0f_{5/2}^{-2})_2(0g_{9/2}^2)_8]\nu(1d_{5/2}^2)_0$	4	28
11_1^+	$\pi[(0f_{5/2}^{-2})_0(0g_{9/2}^2)_8]\nu(1d_{5/2}^2)_4$	4	14
12_1^+	$\pi[(0f_{5/2}^{-2})_0(0g_{9/2}^2)_8]\nu(1d_{5/2}^2)_4$	4	20
13_1^+	$\pi[(0f_{5/2}^{-1}1p_{3/2}^{-1})_2(0g_{9/2}^2)_8]\nu(1d_{5/2}^2)_4$	6	22
14_1^+	$\pi[(0f_{5/2}^{-2})_2(0g_{9/2}^2)_8]\nu(1d_{5/2}^2)_4$	6	52
14_2^+	$\pi[(0f_{5/2}^{-1}1p_{3/2}^{-1})_2(0g_{9/2}^2)_8]\nu(1d_{5/2}^2)_4$	6	15
15_1^+	$\pi[(0f_{5/2}^{-2})_4(0g_{9/2}^2)_8]\nu(1d_{5/2}^2)_4$	6	35
16_1^+	$\pi[(0f_{5/2}^{-2})_4(0g_{9/2}^2)_8]\nu(1d_{5/2}^2)_4$	6	52

[a]Main contribution to the wave function.
[b]Seniority.
[c]Contribution in percent.

TABLE V. Main components of wave functions of negative-parity states in ^{90}Sr.

J^{π}	Configuration[a]	v[b]	A[c]
3_1^-	$\pi(1p_{3/2}^{-1}0g_{9/2}^1)_3\nu(1d_{5/2}^2)_0$	2	42
4_1^-	$\pi(0f_{5/2}^{-1}0g_{9/2}^1)_4\nu(1d_{5/2}^2)_0$	2	26
5_1^-	$\pi(1p_{3/2}^{-1}0g_{9/2}^1)_5\nu(1d_{5/2}^2)_0$	2	31
5_2^-	$\pi(1p_{3/2}^{-1}0g_{9/2}^1)_3\nu(1d_{5/2}^2)_2$	4	32
6_1^-	$\pi(0f_{5/2}^{-1}0g_{9/2}^1)_6\nu(1d_{5/2}^2)_0$	2	43
7_1^-	$\pi(1p_{3/2}^{-1}0g_{9/2}^1)_3\nu(1d_{5/2}^2)_4$	4	54
7_2^-	$\pi(0f_{5/2}^{-1}0g_{9/2}^1)_6\nu(1d_{5/2}^2)_2$	4	31
	$\pi(0f_{5/2}^{-1}0g_{9/2}^1)_7\nu(1d_{5/2}^2)_0$	2	22
7_3^-	$\pi(0f_{5/2}^{-1}0g_{9/2}^1)_4\nu(1d_{5/2}^2)_4$	4	16
8_1^-	$\pi(0f_{5/2}^{-1}0g_{9/2}^1)_4\nu(1d_{5/2}^2)_4$	4	30
8_2^-	$\pi(0f_{5/2}^{-1}0g_{9/2}^1)_6\nu(1d_{5/2}^2)_2$	4	22
9_1^-	$\pi(0f_{5/2}^{-1}0g_{9/2}^1)_6\nu(1d_{5/2}^2)_4$	4	33
9_2^-	$\pi(1p_{3/2}^{-1}0g_{9/2}^1)_5\nu(1d_{5/2}^2)_4$	4	31
10_1^-	$\pi(0f_{5/2}^{-1}0g_{9/2}^1)_6\nu(1d_{5/2}^2)_4$	4	65
11_1^-	$\pi(0f_{5/2}^{-1}0g_{9/2}^1)_7\nu(1d_{5/2}^2)_4$	4	66
12_1^-	$\pi[(0f_{5/2}^{-1}1p_{3/2}^{-1})_4(1p_{1/2}^1 0g_{9/2}^1)_5]\nu(1d_{5/2}^2)_4$	6	69
13_1^-	$\pi[(0f_{5/2}^{-1}1p_{3/2}^{-1})_4(1p_{1/2}^1 0g_{9/2}^1)_5]\nu(1d_{5/2}^2)_4$	8	74
14_1^-	$\pi[(0f_{5/2}^{-2}1p_{3/2}^{-1})(0g_{9/2}^3)]\nu(1d_{5/2}^2)_4$	8	7

[a]Main contribution to the wave function.
[b]Seniority.
[c]Contribution in percent.

TABLE VI. Experimental and calculated transition strengths in ^{90}Sr.

	J_i^{π}	J_f^{π}	$B(E2)_{EXP}$ [a] (W.u.)	$B(E2)_{SM}$ [b] (W.u.)
^{90}Sr	2_1^+	0_1^+	$8.5_{-1.9}^{+3.7}$ [c]	9.7
	4_1^+	2_1^+	$5.3_{-0.8}^{+1.1}$ [c]	5.5

[a]Experimental reduced transition strengths in Weisskopf units (W.u.). 1 W.u.$(E2)=23.96e^2\mathrm{fm}^4$.
[b]Calculated reduced transition strengths in Weisskopf units. Values of $e_{\pi}=1.72e, e_{\nu}=1.44e$ were used for the $B(E2)$.
[c]Value derived from the lifetime given in Ref. [1].

$$\pi[(0f_{5/2}^{-1}1p_{3/2}^{-1})_2(0g_{9/2}^2)_8]\nu(1d_{5/2}^2)_4$$

or

$$\pi[(0f_{5/2}^{-2})_{J_f}(0g_{9/2}^2)_8]\nu(1d_{5/2}^2)_4$$

with $J_f=2,4$. The level spacings between the experimental 0^+, 2^+, and 4^+ states and between the experimental 8^+, 10^+, and 12^+ states are very similar, which may indicate that the 10^+ and 12^+ states are generated by coupling the 2_1^+ and 4_1^+ states, respectively, to the 8^+ state. A similar coupling was discussed in the $N=52$ isotone ^{92}Zr [38]. The configurations of the calculated states predict indeed such a coupling for the 8^+ and 12_1^+ states ($J_f=0$, $J_g=8$, and $J_d=0,4$, respectively), while it is different for the 10_1^+ state ($J_f=0$,

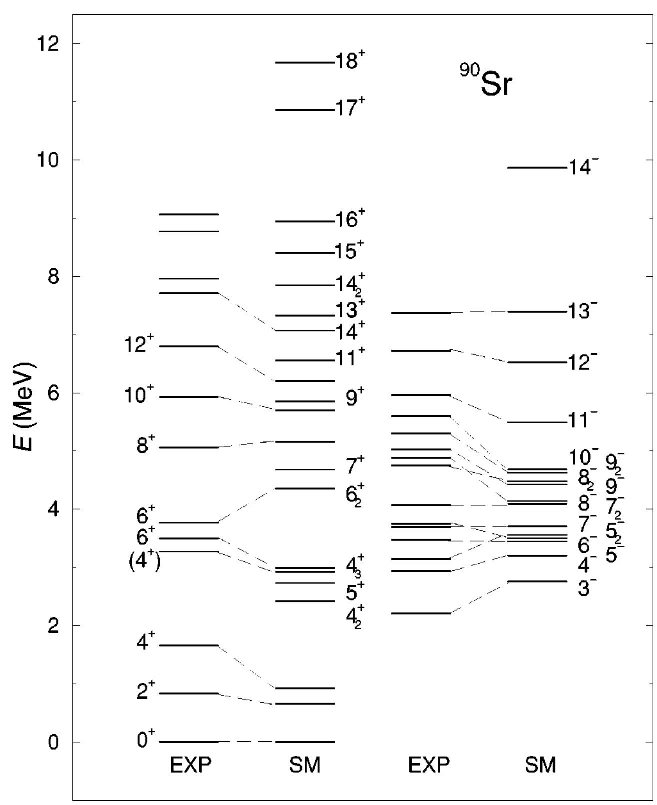

FIG. 7. Comparison of experimental with calculated level energies in ^{90}Sr.

$J_g=6$, and $J_d=4$). As a result, the calculated states with even spins are energetically favored with respect to the states with odd spins. This is consistent with the experiment, where states with odd spins were not observed. Our calculations predict $B(E2)$ values of 9 and 12 W.u. for the $10_1^+\to 8_1^+$ and $12^+\to 10_1^+$ transitions, respectively, which are similar to the transition strengths between the $0^+,2^+,4^+$ states (cf. Table VI) and agree with the discussed coupling scheme. In contrast, small values of $B(E2)\approx 3$ and 0.2 W.u. are calculated for the $10_2^+\to 8^+$ and $12^+\to 10_2^+$ transitions, respectively. Therefore, the experimental state at 5923 keV may be related with the calculated 10_1^+ state. The experimental 7706 keV state may correspond to the calculated 14_1^+ state. A relatively weak transition strength of 4 W.u. is calculated for the $14^+\to 12^+$ transition. In summary, the equidistant $\Delta J=2$ level sequence on top of the 8^+ state, which resembles a vibrational-like sequence, is well reproduced by the present shell-model calculations. The levels above the 7706 keV state might correspond to the calculated higher-spin positive-parity states.

The calculated lowest-lying negative-parity states with $3\leqslant J\leqslant 6$ are dominated by the configurations $\pi(1p_{3/2}^{-1}0g_{9/2}^{1})\nu(1d_{5/2}^{2})_0$ or $\pi(0f_{5/2}^{-1}0g_{9/2}^{1})\nu(1d_{5/2}^{2})_0$, while the calculated second states with $4\leqslant J\leqslant 6$ are dominated by the configuration $\pi(1p_{3/2}^{-1}0g_{9/2}^{1})_3\nu(1d_{5/2}^{2})_{J_d}$ with $J_d=2,4$. The calculated 3_1^-, 4_1^-, 5_1^-, 5_2^-, and 6_1^- states may correspond to the experimental levels at 2207, 2928, 3468, 3144, and 3742 keV, respectively. A main configuration of $\pi(1p_{3/2}^{-1}0g_{9/2}^{1})_3\nu(1d_{5/2}^{2})_4$ was obtained for the first 7^- state in the present calculations that is analogous to $\pi(1p_{3/2}^{-1}0g_{9/2}^{1})_3\nu(1d_{5/2}^{1})$ for the $11/2^-$ state in ^{89}Sr (see Sec. III B). Both states are depopulated by $E3$ transitions with very close energies of 2042.6 and 2079.4 keV, respectively. The calculations predict higher values of 2782 and 2777 keV, respectively, approaching the experimental energy of the 3^- state at 2734 keV in ^{88}Sr [2]. Accordingly, the lowest 3^- state is calculated at approximately the same energy of 2751 keV, i.e., about 500 keV higher than the experimental one. In a previous (d,p) study [36] an admixture of the $\nu(0h_{11/2})$ orbital in the $11/2^-$ state in ^{89}Sr is considered to lower its energy (see Sec. III B). Because of the comparable experimental and calculated energies of the discussed $E3$ transitions such an effect may also be assumed for the experimental 3^- state, and consequently also for the 7^- state in ^{90}Sr. On the other hand, states including the coupling of the two unpaired $(1d_{5/2}^{2})_4$ neutrons to proton excitations are calculated too low as discussed above for the positive-parity states. Besides the considered 7^- state, this holds for most of the negative-parity states with $J>6$ (cf. Fig. 7 and Table V) as well. Due to the discussed shift of the calculated energy of the 3^- and 7^- states the calculated 5_2^- state having an analogous proton configuration may be calculated too high as well. Therefore, the 5_2^- state may be related with the experimental state at 3144 keV, while the calculated 5_1^- state may correspond to the experimental state at 3468 keV.

The calculated lowest-lying 8^- to 11^- states are dominated by the $\pi(0f_{5/2}^{-1}0g_{9/2}^{1})\nu(1d_{5/2}^{2})_4$ configuration, while the second 8^- and 9^- states are dominated by configurations $\pi(0f_{5/2}^{-1}0g_{9/2}^{1})\nu(1d_{5/2}^{2})_2$ and $\pi(1p_{3/2}^{-1}0g_{9/2}^{1})\nu(1d_{5/2}^{2})_4$, respectively. The equidistant level spacings between the 4066, 5022, and 5961 keV levels are similar to the level spacings between the first 0^+, 2^+, and 4^+ states, which might suggest that the $9^{(-)}$ and $11^{(-)}$ states at 5022 and 5961 keV, respectively, result from coupling the first 2^+ and 4^+ states to the $7^{(-)}$ state at 4066 keV, respectively. In this case, the configuration $\pi(0f_{5/2}^{-1}0g_{9/2}^{1})_7\nu(1d_{5/2}^{2})_{J_d}$ with $J_d=0,2,4$ should dominate the 4066, 5022, and 5961 keV levels, respectively. The present calculations predict such a configuration as main component for the first 11^- state as well as a significant contribution to the second calculated 7^- state, but not for the lowest three 9^- states. Considering the shift of the energies of states generated by coupling the $\nu(1d_{5/2}^{2})_4$ configuration to proton excitations, we consider the calculated 8_2^-, 8_1^-, 9_2^-, 10_1^-, and 11_1^- states to correspond to the experimental states at 4749, 4882, 5298, 5592, and 5961 keV, respectively. To generate 12^- and 13^- states a second proton pair is broken and two protons are lifted over the shell gap at $Z=38$. The main configuration of these states is $\pi(0f_{5/2}^{-1}1p_{3/2}^{-1}1p_{1/2}^{1}0g_{9/2}^{1})\nu(1d_{5/2}^{2})_4$. The 14^- state is generated by lifting three protons over the shell gap at $Z=38$. Accordingly, a gap of about 2.5 MeV is predicted between the calculated 13^- state and the 14^- state, which has no counterpart in our experiment.

IV. SUMMARY

High-spin states of ^{89}Sr and ^{90}Sr were studied via the reactions ^{82}Se(^{11}B, $p3n$) and ^{82}Se(^{11}B, $p2n$), respectively, at a beam energy of 37 MeV with the GASP spectrometer. The level schemes of ^{89}Sr and ^{90}Sr were extended up to 8 MeV and 10 MeV, respectively. On the basis of DCO ratios spin assignments for six newly observed states in ^{89}Sr and for most of the states in ^{90}Sr above the 4^+ level at 1656 keV were made for the first time. Excited states in ^{89}Sr and ^{90}Sr were interpreted in the framework of the shell model. The calculations were performed in a model space including the $(0f_{5/2},1p_{3/2},1p_{1/2},g_{9/2})$ orbitals for the protons and the $(1p_{1/2},0g_{9/2},1d_{5/2})$ orbitals for the neutrons. Based on these calculations the states up to $27/2^+$ and $23/2^-$, respectively, in ^{89}Sr can be regarded as generated by coupling a $1d_{5/2}$ neutron to proton states in the core nucleus ^{88}Sr. The 6857 keV state cannot be described with the present calculations. This feature suggests the possible influence of a $0g_{7/2}$ neutron. The present calculations for ^{90}Sr give a good overall description of the observed states. The comparison of the experimental with the calculated states does not indicate noticeable quenching of the $p_{3/2}-p_{1/2}$ proton spin-orbital splitting in ^{90}Sr. The observed equidistant $\Delta J=2$ level sequence on top of the 8^+ state, which resembles a vibrational-like structure, could be well described by the configuration $\pi[(0f_{5/2}^{-2})(0g_{9/2}^{2})]\nu(1d_{5/2}^{2})$ favoring even spins.

ACKNOWLEDGMENTS

This work was supported by the European Union within the TMR-LSF program under Contract No. ERBFMGECT980110. E.A.S. acknowledges financial support by the Sächsisches Staatsministerium für Wissenschaft und Kunst under Contract No. SMWK/4-7531.50-04-844-00/21 and by the Bulgarian NRF under Contract No. PH 908. T.K. acknowledges EC financial support under TMR Contract No. ERBFMRXCT97-0123.

[1] H. Mach, F. K. Wohn, G. Molnŕ, K. Sistemich, J. C. Hill, M. Moszyński, R. L. Gill, W. Krips, and D. S. Brenner, Nucl. Phys. **A523**, 197 (1991).
[2] H. W. Müller and J. W. Tepel, Nucl. Data Sheets **54**, 1 (1988).
[3] H. Mach, M. Moszyński, R. L. Gill, F. K. Wohn, J. A. Winger, J. C. Hill, G. Molnár, and K. Sistemich, Phys. Lett. B **230**, 21 (1989).
[4] P. Federman, S. Pittel, and A. Etchegoyen, Phys. Lett. **140B**, 269 (1984).
[5] E. A. Stefanova, R. Schwengner, J. Reif, H. Schnarez, F. Dönau, M. Wilhelm, A. Fitzler, S. Kasemann, P. von Brentano, and W. Andrejtscheff, Phys. Rev. C **62**, 054314 (2000).
[6] S. E. Arnell, A. Nilsson, and O. Stankiewicz, Nucl. Phys. **A241**, 109 (1975).
[7] E. Wallander, A. Nilsson, L. P. Eksröm, G. D. Jones, F. Kearns, T. P. Morrison, H. G. Price, P. J. Twin, R. Wadsworth, and N. J. Ward, Nucl. Phys. **A361**, 387 (1981).
[8] W. L. Talbert, F. K. Wohn, L. J. Alquist, and C. L. Duke, Phys. Rev. C **23**, 1726 (1981).
[9] E. R. Flynn, Ole Hansen, J. D. Sherman, Nelson Stein, and J. W. Sunier, Nucl. Phys. **A264**, 253 (1976).
[10] R. S. Tickle, W. S. Gray, and R. D. Bent, Nucl. Phys. **A376**, 309 (1982).
[11] N. Fotiades, J. A. Cizewski, K. Y. Ding, R. Krücken, J. A. Becker, L. A. Bernstein, K. Hauschild, D. P. McNabb, W. Younes, P. Fallon, I. Y. Lee, and A. O. Macchiavelli, in *Proceedings of the International Conference on Achievements and Perspectives in Nuclear Structure, Aghia Palaghia, Greece, 1999*, edited by S. Åberg and C. Kalfas [Phys. Scr. **T88**, 127 (2000)].
[12] D. Bazzacco, in *International Conference on Nuclear Structure at High Angular Momentum*, Ottawa, 1992, Chalk River Report (AECL 10613), p. 386.
[13] A. Gavron, Phys. Rev. C **21**, 230 (1980).
[14] D. C. Radford, Nucl. Instrum. Methods Phys. Res. A **361**, 297 (1995).
[15] J. Theuerkauf, S. Esser, S. Krink, M. Luig, N. Nicolay, and H. Wolters, Program VS (version 6.65), Universität zu Köln, 1992.
[16] R. M. Steffen and K. Alder, in *The Electromagnetic Interaction in Nuclear Spectroscopy*, edited by W. D. Hamilton (North-Holland, Amsterdam, 1975), p. 505.
[17] K. S. Krane, R. M. Steffen, and R. M. Wheeler, Nucl. Data Tables **11**, 351 (1973).
[18] A. Krämer-Flecken, T. Morek, R. M. Lieder, W. Gast, G. Hebbinghaus, H. M. Jäger, and W. Urban, Nucl. Instrum. Methods Phys. Res. A **275**, 333 (1989).
[19] E. Cosman, D. Slater, R. F. Casten, E. R. Flynn, and O. Hansen, Phys. Rev. C **10**, 671 (1974).
[20] S. S. Ghugre, S. Naguleswaran, R. K. Bhowmik, U. Garg, S. B. Patel, W. Reviol, and J. C. Walpe, Phys. Rev. C **51**, 2809 (1995).
[21] S. S. Ghugre, S. B. Patel, M. Gupta, R. K. Bhowmik, and J. A. Sheikh, Phys. Rev. C **50**, 1346 (1994).
[22] B. Kharraja, S. S. Ghugre, U. Garg, R. V. F. Janssens, M. P. Carpenter, B. Crowell, T. L. Khoo, T. Lauritsen, D. Nisius, W. Reviol, W. F. Mueller, L. L. Riedinger, and R. Kaczarowski, Phys. Rev. C **57**, 2903 (1998).
[23] B. Kharraja, S. S. Ghugre, U. Garg, R. V. F. Janssens, M. P. Carpenter, B. Crowell, T. L. Khoo, T. Lauritsen, D. Nisius, W. Reviol, W. F. Mueller, L. L. Riedinger, and R. Kaczarowski, Phys. Rev. C **57**, 83 (1998).
[24] G. Winter, R. Schwengner, J. Reif, H. Prade, L. Funke, R. Wirowski, N. Nicolay, A. Dewald, P. von Brentano, H. Grawe, and R. Schubart, Phys. Rev. C **48**, 1010 (1993).
[25] G. Winter, R. Schwengner, J. Reif, H. Prade, J. Döring, R. Wirowski, N. Nicolay, P. von Brentano, H. Grawe, and R. Schubart, Phys. Rev. C **49**, 2427 (1994).
[26] R. Schwengner, G. Winter, J. Reif, H. Prade, L. Käubler, R. Wirowski, N. Nicolay, S. Albers, S. Eßer, P. von Brentano, and W. Andrejtscheff, Nucl. Phys. **A584**, 159 (1995).
[27] R. Schwengner, J. Reif, H. Schnare, G. Winter, T. Servene, L. Käubler, H. Prade, M. Wilhelm, A. Fitzler, S. Kasemann, E. Radermacher, and P. von Brentano, Phys. Rev. C **57**, 2892 (1998).
[28] X. Ji and B. H. Wildenthal, Phys. Rev. C **37**, 1256 (1988).
[29] R. Gross and A. Frenkel, Nucl. Phys. **A267**, 85 (1976).
[30] P. C. Li, W. W. Daehnick, S. K. Saha, J. D. Brown, and R. T. Kouzes, Nucl. Phys. **A469**, 393 (1987).
[31] J. Blomqvist and L. Rydström, Phys. Scr. **31**, 31 (1985).
[32] D. H. Gloeckner and F. J. D. Serduke, Nucl. Phys. **A220**, 477 (1974).
[33] D. Zwarts, Comput. Phys. Commun. **38**, 365 (1985).
[34] T. E. Milliman, J. H. Heisenberg, F. W. Hersman, J. P. Connelly, C. N. Papanicolas, J. E. Wise, H. P. Blok, and L. T. van der Bijl, Phys. Rev. C **32**, 805 (1985).
[35] C. A. Heras and S. M. Abecasis, Z. Phys. A **324**, 403 (1986).
[36] H. P. Blok, W. R. Zimmerman, J. J. Kraushaar, and P. A. Batay-Csorba, Nucl. Phys. **A287**, 156 (1987).
[37] H. Mach, E. K. Warburton, W. Krips, R. L. Gill, and G. Molnár, Phys. Rev. C **42**, 568 (1990).
[38] B. A. Brown, D. B. Fossan, P. M. S. Lesser, and A. R. Poletti, Phys. Rev. C **14**, 602 (1976).
[39] B. Singh, Nucl. Data Sheets **85**, 1 (1998).